Organic Selenocyanates as Halide Receptors: From Chelation to One-Dimensional Systems

Asia Marie S. Riel, Huu-Tri Huynh, Olivier Jeannin, Orion Berryman, Marc Fourmigué

Organic selenocyanates as halide receptors: from chelation to one-dimensional systems

Asia Marie S. Riel,[†,‡] Huu-Tri Huynh,[†] Olivier Jeannin,[†] Orion Berryman,[‡] and Marc Fourmigué*,[†]

[†] Univ Rennes, CNRS, ISCR (Institut de Sciences Chimiques de Rennes), UMR 6226, 35000 Rennes, France

[‡] Department of Chemistry and Biochemistry, University of Montana, 32 Campus Dr., Missoula MT 59812, USA

ABSTRACT

Organic selenocyanates were recently identified as strong chalcogen bond donors. They also play an important role in biochemistry. Here, we show that 1,2-bis(selenocyanatomethyl)benzene **1** and 1,2,4,5-tetrakis(selenocyanatomethyl)-benzene **2** crystallize from DMF to afford solvates where two *ortho* SeCN moieties act as a chelate toward the carbonyl oxygen atom of DMF through strong Se•••O chalcogen bonds. This result led us to explore their ability to also chelate halide anions (Cl⁻, Br⁻) in solution as well as in the solid state, an important issue in view of applications in crystal engineering or organocatalysis. NMR titration experiments provide an association constant between **1** and Cl⁻ of 148 M⁻¹. We also observed the recurrent formation of cocrystal salts from the association of the ChB donors **1** and **2** with the onium salts Ph$_4$PCl, Ph$_4$PBr and Bu$_4$NCl. We demonstrate that not only μ_2-halide but also μ_4-halide structures can be stabilized though ChB interactions, leading to the formation of complex polymeric anionic networks. Continuous shape measure calculations of these μ_4-halide structures demonstrate that seesaw symmetry best describes the μ_4-Br⁻ bromide structures, while the smaller chloride anions tend to favor a close-to-tetrahedral μ_4-Cl⁻ organization, which is also confirmed by DFT calculations. Electrostatic surface potential calculations further demonstrate the efficiency of this chelating *ortho*-bis(selenocyanatomethyl) motif in **1** and **2**, with $V_{s,max}$ values reaching 50 kcal mol⁻¹, to be compared with the simplest benzyl selenocyanate (36.4 kcal mol⁻¹) or the reference halogen bond donor F$_5$C$_6$–I (35.7 kcal mol⁻¹) in the same conditions.

INTRODUCTION

The study of the halogen bond (XB) in chemistry is currently developing very actively, with numerous implications in crystal engineering, catalysis, molecular materials or biochemistry.[1,2] With similar characteristics to the XB, the fields of chalcogen, pnictogen and tetrel bonding are also rapidly evolving.[3] For example, properly activated chalcogen atoms (S, Se, Te) can, similarly to halogen atoms, exhibit σ-holes that facilitate a so-called chalcogen bond (ChB) interaction with Lewis bases. Although a ChB has yet no formal definition,[4] it can also be regarded as an attractive and directional noncovalent interaction between an electron-deficient chalcogen (partial positive) and an electron rich Lewis base (partial negative). Theoretical investigations show that in contrast to halogen atoms,[5,6,7] the chalcogen atom can potentially provide two σ-holes, each of them along the C–Ch bonds. Recent results show also that the situation is not that simple and that the location of the maximum ($V_{s,max}$) of the electrostatic surface potential (ESP) on the chalcogen atom can present large deviations from the C–Ch bond axis.[8] Because of these deviations and the emergence of two σ-holes, interaction predictability becomes more difficult and applications of ChB in crystal engineering are scarce. Many examples reporting ChB in crystalline compounds[9] are essentially limited to "amphoteric" symmetric molecules having both ChB donor and acceptor moieties. Examples of these include the earlier structures of $Se(CN)_2$, $Te(CN)_2$ (Scheme 1a-b),[10,11] telluradiazole derivatives (Scheme 1e) [12,13] and selenophthalic anhydride (Scheme 1d).[14] One efficient strategy to potentially favor one σ-hole over the other is to substitute the chalcogen atom with only one strong electron-withdrawing group (EWG), as for example with cationic imidazolium (Scheme 1h) or with nitrile substituents. In that respect, organic selenocyanates R–Se–C≡N were shown to recurrently associate in the solid state through strong Se•••N≡C ChBs generating infinite one-dimensional motifs.[15] Furthermore, their ability to form cocrystals upon interaction with Lewis bases was also demonstrated in the formation of 1:1 adducts between 1,3- or 1,4-bis(selenocyanatomethyl)benzene and 4,4'-bipyridine,[16] leading to the formation of heterochains similar to 1,3- or 1,4-diiodotetrafluorobenzene with the same ditopic 4,4'-bipyridine.[17,18] It should also be stressed that such organic selenocyanates have received wide attention for their biological activity.[19,20,21] Their mode of action is not known but most probably involves a preliminary nucleophilic attack on the Se atom through intermediate ChB-stabilized adducts with the nucleophile.
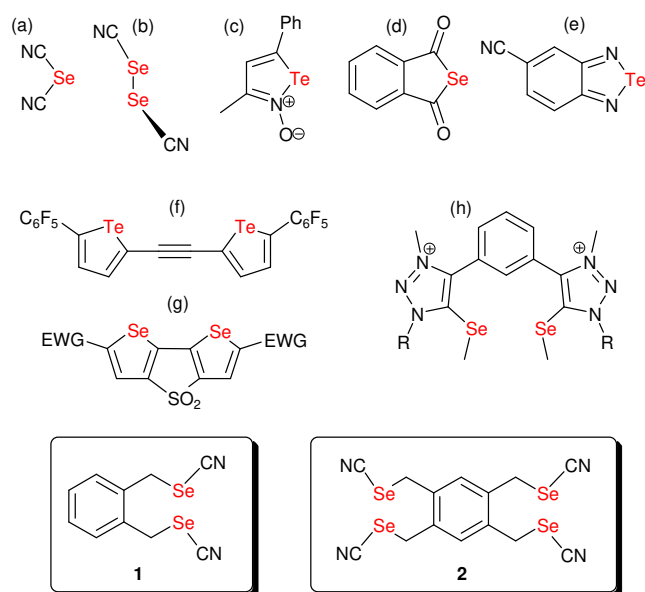
Scheme 1. Selected chalcogen bond (ChB) donors

Besides neutral XB acceptors such as pyridines, σ-hole based interactions with halides has also been the subject of numerous investigations, as the XB interactions are reinforced through charge assistance.[22,23,24,25,26,27] A coordination chemistry of anions can thus be defined[28,29,30,31,32,33,] with coordination numbers up to eight, i.e. eight iodine or bromine atoms of XB donors around one single μ_8-halide anion. A similar "coordination" chemistry of halides through ChB is still in its infancy. It has been originally evaluated only in solution from the evolution of the optical spectrum and/or the NMR signals of ChB donors such as dithienylthiophenes (Scheme 1g)[34] or benzotelluradiazoles (Scheme 1e).[35] The formation of the μ_1- or μ_2-halide adducts, further rationalized through theoretical calculations,[36,37] can be used for anion transport across lipid bilayers,[38,39] a concept extended to oligodithienylthiophene derivatives.[40] Also in solution, neutral rotaxanes incorporating SeMe moieties, as ChB donors, were used to reveal the local electronic environment of the chalcogen atoms in mechanically bonded rotaxane binding sites.[41] Another important emerging application of ChB paralleling the work already reported with XB is catalysis. Indeed the dithienylthiophenes mentioned above were also used to activate the transfer hydrogenation of quinolines and imines, involving an initial step where the two conformationally-locked chalcogen atoms activate the pyridinic nitrogen atoms of the substrate.[42] This work was further extended to another series of ChB donors, namely neutral benzodiselenazole derivatives.[43] Similarly, in the solvolysis of benzhydryl bromide[42,44] or 1-chloroisochroman,[45] considered as

3

halide abstraction benchmark reactions, ChB donors based on bis(benzimidazolium) cores accelerated reactions by a factor of 10-30 relative to the background reaction. Again here, the initial step is based on the interaction of the chalcogen with the electron-rich bromine or chlorine atoms.

It therefore appears at this stage that ChB interactions with halides, demonstrated from solution studies or theoretically investigated, are furthermore limited to μ_1- or μ_2-halide motifs and have rarely been structurally identified and characterized. A CSD search based on non-bonding distances between halide anions (Cl$^-$, Br$^-$, I$^-$) and selenium atoms provides only examples of selenium-containing *cationic* molecules. The only reported, crystallographically characterized examples which can be described as a neutral ChB donor interacting with halides is the association between selenocyanogen NCSe–SeCN and PhNMe$_3$$^+Br^-$ to give the μ_1-Br$^-$ complex,[46] or very recently the association of 1,2,5-chalcogenadiazoles (Te, Se, S) with pseudo halides.[47]

As mentioned above, we recently reported that organic selenocyanates such as **1** and **2** (Scheme 1) crystallize with recurrent formation of chains stabilized through intermolecular Se•••NC ChB interactions. Furthermore, recrystallization of **2** from DMF afforded a bis adduct where two neighboring SeCN moieties act as a chelate toward the carbonyl oxygen atom of DMF. We found (see below) that the very same process takes place with the *ortho* derivative **1**. We therefore considered that such *ortho*-substituted bis(selenocyanotomethyl) derivatives **1** or **2** could be well adapted to the chelation of halide anions, an interesting issue in view of their easy synthesis, and their possible applications in crystal engineering or organocatalysis (see above), as very recently reported by Bryce *et al*. from solution NMR and solid state studies.[48]

We report here on the formation of cocrystal salts from the association of the ChB donors **1** and **2** with the onium salts Ph$_4$PCl, Ph$_4$PBr and Bu$_4$NCl, demonstrating their ability to chelate halide anions though ChB interactions. Furthermore, we demonstrate here that not only μ_2-halide but also μ_4-halide structures can be stabilized though ChB interactions, leading to the formation of polymeric anionic networks.

4

RESULTS AND DISCUSSION

The two ChB donors **1** and **2** were prepared from the reaction of the corresponding bromomethyl derivatives with KSeCN, as described earlier.[15] Recrystallization from DMF was shown to form the bis(DMF) adduct with **2**, a similar monoadduct is obtained with **1**. This solvate **1**•DMF crystallizes in the monoclinic system, space group $P2_1/a$, with one molecule in the general position within the unit cell. As shown in Figure 1a and Table 1, the Se•••O interaction is short: the reduction ratio (RR), defined as the ratio of the actual distance over the sum of van der Waals radii, amounts to 0.90. Furthermore, the C–Se•••O angles are close to 180° demonstrating the strong directionality of the interactions. The striking difference between the two DMF adducts is the relative conformation of the SeCN moieties relative to the aromatic plane. They adopt an *anti* conformation in **1**•DMF (Figure 1a) with a Se•••O•••Se angle of 101.4(1)°, while a *syn* conformation with a very acute Se•••O•••Se angle of 79.2(1)° was found in **2**•(DMF)$_2$ (Figure 1b) which brings the two Se atoms at van der Waals contact (3.75 Å). These two DMF adducts demonstrate not only the ability of this motif to chelate but also its flexibility as it can adopt both *syn* and *anti* conformations, with an even stronger interaction in the *syn* conformation. The cocrystallization of **1** and **2** with tetraphenylphosphonium and tetrabutylammonium halides was therefore undertaken to evaluate their ability to also interact and chelate halide anions, with the added possibility to form extended one-dimensional motifs.
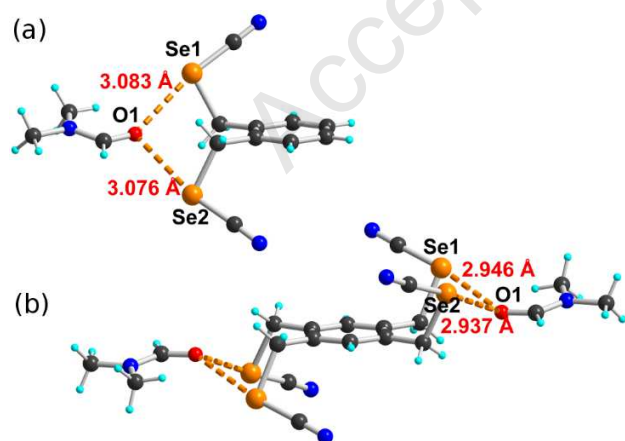

Figure 1. Detail of the DMF adducts, (a) **1**•DMF, and (b) **2**•(DMF)$_2$.

Table 1. Structural characteristics of the ChB interactions in the DMF adducts of **1** and **2**.

Conpound	Interaction	Se•••N (Å)	RR	C–Se•••N (°)	Ref.
1•(DMF)	Se1•••O	3.083(5)	0.90	168.9(2)	this work
	Se2•••O	3.076(5)	0.90	168.4(2)	
2•(DMF)$_2$	Se1•••O	2.95(12)	0.86	171.9(2)	15
	Se2•••O	2.94(5)	0.86	175.2(2)	

Accordingly, **1** and **2** were associated with the chloride and bromide salts of Ph_4P^+ and n-Bu_4N^+ as cations. Several co-crystal salts were obtained, with different stoichiometry, formulated as (**1**)$_2$•PPh$_4$Cl•Et$_2$O, (**1**)$_2$•PPh$_4$Br, **2**•(PPh$_4$Cl)$_2$, **2**•(PPh$_4$Br)$_2$, and **2**•Bu4NCl. Two other phases obtained in moist conditions and incorporating hydrogen-bonded water molecules, are formulated as **2**•(PPh$_4$Cl)$_2$•(H$_2$O)$_2$ and **2**•(PPh$_4$Br)$_2$•(H$_2$O)$_2$. They are isostructural and are described only in the ESI. The different structures can be separated into two groups, according to the actual number of selenium atoms around the halide anion. We will first describe μ_2-halide structures analogous to those observed with neutral DMF, followed by the μ_4-halide structures.

The μ_2-halide chalcogen-bonded structures. **2**•(PPh$_4$Cl)$_2$ crystallizes in the triclinic $P\bar{1}$ space group, with the tetradentate ChB donor **2** on an inversion center, and Ph$_4$PCl in the general position, hence the stoichiometry. As shown in Figure 2, two neighboring SeCN moieties interact with the Cl$^-$ anion through short and directional ChB, providing a motif which differs from the DMF solvate by the *anti* orientation of the two SeCN moieties. Structural characteristics are collected in Table 2. Note that the chloride is otherwise surrounded only by hydrogen atoms at van der Waals contacts. This first example already demonstrates the flexibility of the ChB donors reported here, since in its DMF adduct, a *syn* orientation of the neighboring SeCN moieties was observed, in contrast with the *anti* orientation found here. Note also the Se$_1$•••Cl$^-$•••Se$_2$ angle found here at 93.40(3)°, which is notably smaller than the angle found in the *anti* configuration of **1**•DMF (Figure 1a), a possible consequence of the slightly larger Se•••Cl$^-$ distances when compared with the Se•••O ones.
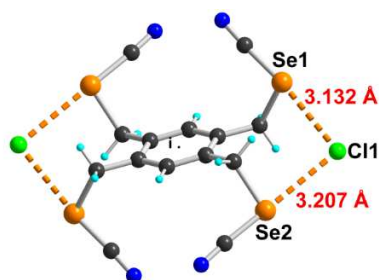
Figure 2. Detail of the interaction between **2** and Cl^- in **2**•(PPh$_4$Cl)$_2$

Table 2. Structural characteristics of the ChB interactions in μ_2-halide structures in the cocrystals salts with **2**. The ionic radii (rather than the van der Waals radii) were used for Cl^- (1.81 Å) and Br^- (1.96 Å).

| Compound	Interaction	Se•••Cl/Br (Å)	RR	C–Se•••Cl/Br (°)
2•(PPh$_4$Cl)$_2$	Se$_1$•••Cl	3.132(5)	0.844	173.3(2)
	Se$_2$•••Cl	3.207(8)	0.864	173.9(2)
2•(PPh$_4$Br)$_2$	Se$_1$•••Br	3.23(1)	0.837	176.8(3)
	Se$_2$•••Br	3.25(1)	0.842	174.6(3)

Unexpectedly, the analogous Ph$_4$PBr bromide salt, albeit precipitating with the same stoichiometry, i.e. **2**•(PPh$_4$Br)$_2$, gives a completely different pattern. It crystallizes in the triclinic system, space group $P\bar{1}$, with the ChB donor molecule **2** on an inversion center and PPh$_4$Br in the general position in the unit cell. As shown in Figure 3, the bromide is still interacting with two Se atoms but from two different ChB donor molecules **2**, giving rise to complex anionic chains running along the crystallographic *a* axis. However, structural characteristics of the ChB interactions (Table 2) are similar to those observed in the Cl^- salt, with the only difference being the smaller Se$_1$•••Br$^-$•••Se$_2$ angle at 83.44(3)°.
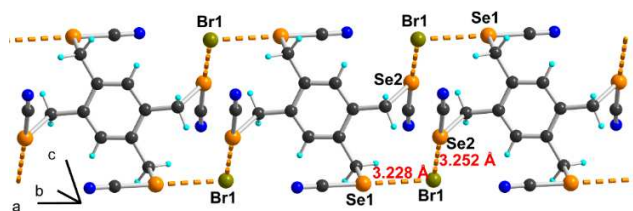
Figure 3. Detail of the ChB chains running along *a* in **2**•(PPh$_4$Br)$_2$.

The μ4-halide chalcogen-bonded structures. The tetraphenylphosphonium salts with the *ortho*-substituted ChB donor molecule **1** were isolated with a different stoichiometry than **2**, i.e. (**1**)$_2$•PPh$_4$Cl•Et$_2$O and (**1**)$_2$•PPh$_4$Br, corresponding therefore to four SeCN group for each halide anion, i.e. a μ$_4$-halide coordination. The Cl$^-$ salt (**1**)$_2$•PPh$_4$Cl•Et$_2$O crystallizes in the monoclinic system, space group P2$_1$/n, with two crystallographically independent ChB donor molecules **1**, as well as the PPh$_4$Cl in the general position in the unit cell, with an added Et$_2$O molecule. The Cl$^-$ is interacting here with four selenium atoms through short and directional ChB contacts (Figure 4a, Table 3). One of the four ChB distances is slightly larger than the three others which compare to those found above in **2**•(PPh$_4$Cl)$_2$ where the Cl$^-$ anion was interacting with only two Se atoms. This dissymmetry might indicate either steric constraints which limits a complete four-fold coordination, or a weakening of the ChB interactions, as the monovalent chloride anion is now acting as ChB acceptor toward four rather than two ChB donors. This weakening is actually also observed in the bromide salts, as detailed below.
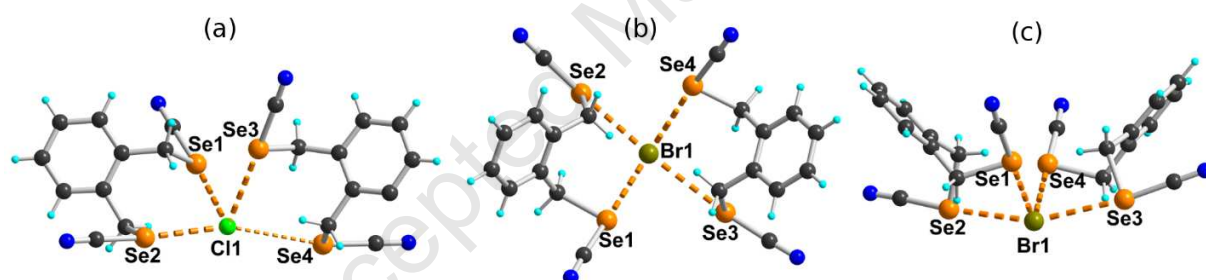
Figure 4. Detail of: (a) the Cl$^-$ and (b,c) the Br$^-$ environment in the crystal structures of (a): (**1**)$_2$•PPh$_4$Cl•Et$_2$O and (b,c): (**1**)$_2$•PPh$_4$Br (orthorhombic phase).

Table 3. Structural characteristics of the ChB interactions in μ_4-halide structures in the cocrystals salts with **1** and **2**. The ionic radii (rather than the van der Waals radii) were used for Cl⁻ (1.81 Å) and Br⁻ (1.96 Å) while a van der Waals radius of 1.90 Å was used for selenium.

| Compound	Interaction	Se•••Cl/Br (Å)	RR	C–Se•••Cl/Br (°)
$(\mathbf{1})_2$•PPh$_4$Cl•Et$_2$O	Se$_1$•••Cl	3.188(2)	0.859	172.6(2)
	Se$_2$•••Cl	3.166(3)	0.853	174.9(2)
	Se$_3$•••Cl	3.220(3)	0.868	179.2(3)
	Se$_4$•••Cl	3.473(4)	0.937	167.7(2)
$(\mathbf{1})_2$•PPh$_4$Br	Se$_1$•••Br	3.363(3)	0.871	177.48(1)
monoclinic phase	Se$_2$•••Br	3.225(10	0.835	174.86(1)
	Se$_3$•••Br	3.358(14)	0.870	173.64(1)
	Se$_4$•••Br	3.552(1)	0.920	172.88(1)
$(\mathbf{1})_2$•PPh$_4$Br	Se$_1$•••Br	3.343(1)	0.866	176.5(1)
orthorhombic phase	Se$_2$•••Br	3.186(1)	0.825	175.4(1)
	Se$_3$•••Br	3.346(1)	0.867	171.9(1)
	Se$_4$•••Br	3.459(1)	0.930	172.6(1)
$\mathbf{2}$•Bu$_4$NCl	Se$_1$•••Cl	3.176(3)	0.856	173.9(2)
	Se$_2$•••Cl	3.162(2)	0.852	171.2(2)
	Se$_3$•••Cl	3.220(4)	0.868	174.7 (3)
	Se$_4$•••Cl	3.202(2)	0.863	[a]
$\mathbf{2}$•Bu$_4$NCl•(PhCN)$_{0.5}$	Se$_1$•••Cl1	3.154(9) (×2)	0.850	169.9 (3)
	Se$_2$•••Cl1	3.140(5) (×2)	0.846	[a]
	Se$_3$•••Cl2	3.092(5) (×2)	0.833	173.0 (3)
	Se$_4$•••Cl2	3.244(7) (×2)	0.874	169.7 (3)

[a] SeCN disordered on two positions

$(\mathbf{1})_2$•PPh$_4$Br was obtained as concomitant polymorphs, one crystallizing in the monoclinic P2$_1$ space group, the other in the orthorhombic P2$_1$2$_1$2$_1$ space group. A very similar motif is observed around the Br⁻ anion (Figure 4b and 4c) in both polymorphs, which differ only by the relative organization of otherwise identical supramolecular layers (Figure S1 in ESI). The

coordination geometry around the Br⁻ is essentially the same in both phases (See Table 3). These structures provide the very first examples of an μ_4-halide anion coordination through ChB donors. They are also characterized by a peculiar organization around the halide, with the four selenium atoms lying in the same hemisphere, with acute Se•••X⁻•••Se angles. Such geometries are in complete opposition to the classical metal coordination chemistry where overlapping interactions of the ligands orbitals with the nd, $(n+1)s$ and $(n+1)p$ orbitals of the metal center, together with the electron count, determines the favored coordination number and geometry, which favors structures where the ligands are farthest apart from each other. This concentration of the chalcogen atoms on one side of the halide, also observed in many instances in XB halide systems, might indicate that the formation of the first XB or ChB interactions with a halide anion, most probably polarizes it to such an extent that the remaining charge is concentrated at the proximity of the first XB or ChB donors, rather than opposite to them (see below).

The μ_4-X⁻ molecular structures obtained above with the bidentate ChB donor **1** let us infer that similar but polymeric μ_4-halide structures should be obtainable from the tetradentate ChB donor **2**. However, cocrystallizations of **2** with PPh₄Cl or PPh₄Br afforded only hydrated phases formulated as **2**•(PPh₄Cl)₂•(H₂O)₂ and **2**•(PPh₄Br)₂•(H₂O)₂ which still exhibit μ_2-halide chalcogen-bonded motifs (See Figures S2, S3 and Table S1 in ESI). On the other hand, attempted cocrystallizations of **2** with the tetrabutylammonium salts n-Bu₄NCl and n-Bu₄NBr afforded crystalline phases with n-Bu₄NCl, actually as two concomitant phases, with one incorporating an extra benzonitrile solvent molecule, but both of them exhibiting these awaited μ_4-X⁻ structures (Figure 5). **2**•Bu₄NCl crystallizes in the monoclinic system, space group P2₁/c, with the tetradentate ChB donor **2** and the tetrabutylammonium salt in the general position in the unit cell. On the other hand, the PhCN solvate **2**•Bu₄NCl•(PhCN)₀.₅ crystallizes in the monoclinic system, space group C2/c, with the ChB donor **2** and the Bu₄N⁺ cation in the general position and two crystallographically independent Cl⁻ anions, each of them located on the two-fold axis along *b*. Note also that in both structures, one CN moiety is disordered over two close positions, with 50:50 occupancy, and that in **2**•Bu₄NCl•(PhCN)₀.₅, the PhCN molecule is disordered on an inversion center. Characteristic bond distances and angles associated with the ChB interactions are collected in Table 3.

10
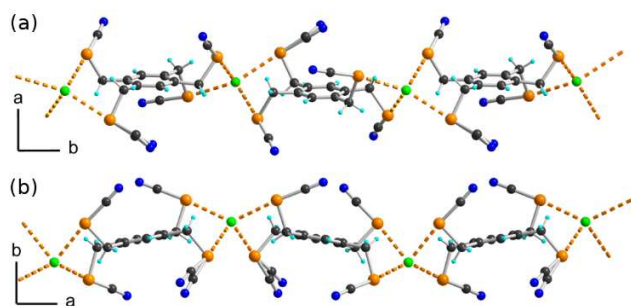
Figure 5. Detail of the chains incorporating the μ_4-Cl$^-$ structures in (a) **2**•Bu$_4$NCl, and (b) **2**•Bu$_4$NCl•(PhCN)$_{0.5}$. Cations and solvent molecules were omitted for clarity.

The six different μ_4-X$^-$ molecular structures described above raise a question relative to the actual geometry around the halide anion. In classical coordination chemistry involving metallic cations at the coordination center, four-fold coordination is mostly represented by tetrahedral (T$_d$ symmetry), and square planar (D$_{4h}$ symmetry) geometries, with a general agreement that metal ions with a d^8 electron configuration prefer the square-planar geometry, whereas d^0 and d^{10} ions are essentially tetrahedral. Such rules are not expected to be obeyed here and indeed we see in Figure 6 that the six structures reported here vary between the tetrahedron and the so-called seesaw (C$_{2v}$) model geometries (Scheme 2), the latter being built from an octahedron with two vacant vertices. A quantitative measure of the proximity of a given geometry to model structures such as tetrahedral or square planar has been reported by Alvarez *et al*.,[49,50] based on the concept of continuous shape/symmetry measure. It is defined as the *distance S(G)* of a molecular structure to the perfect polyhedron belonging to a symmetry point group *G*, with $0 \leq S(G) \leq 100$ with $S(G) = 0$ for the perfect *G* geometry. Analysis of the six structures shown in Figure 6 is reported in Table 4. We note that the smallest $S(G)$ values are actually found with the seesaw symmetry, which describes best the geometry of the μ_4-Br$^-$ bromide structures, while the smaller chloride anions (and shorter Se•••Cl$^-$ distances) tend to favor a close-to-tetrahedral μ_4-Cl$^-$ organization.

11
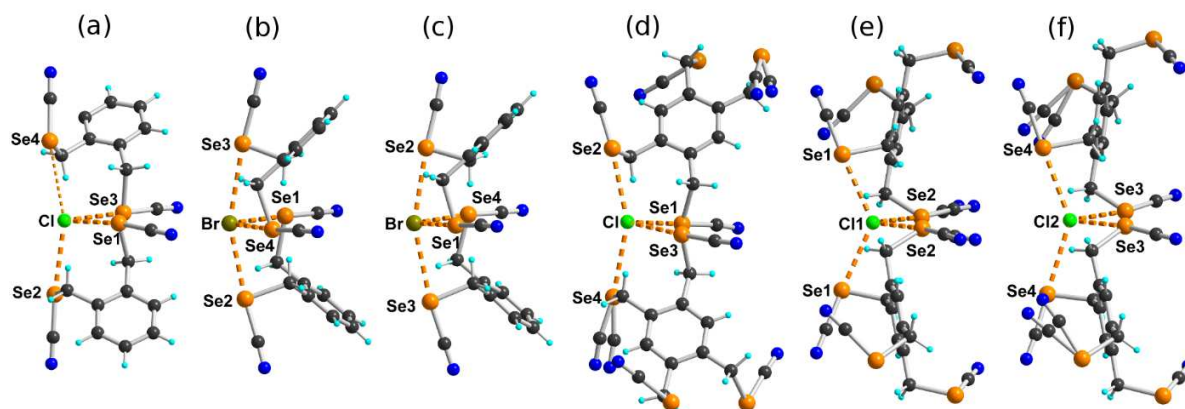
Figure 6. Detail of the μ_4-X$^-$ molecular structures in: (a) (**1**)$_2$•Ph$_4$PCl, (b) (**1**)$_2$•Ph$_4$PBr, monoclinic phase, (c) (**1**)$_2$•Ph$_4$PBr, orthorhombic phase, (d) **2**•Bu$_4$NCl, (e) **2**•Bu$_4$NCl•(PhCN)$_{0.5}$ around Cl(1), (f) **2**•Bu$_4$NCl•(PhCN)$_{0.5}$ around Cl(2).
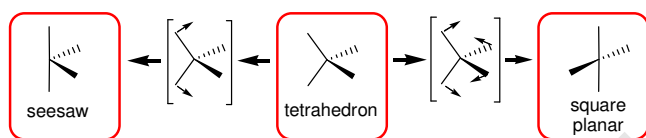
Scheme 2

Preliminary DFT structure optimizations were performed on the μ_4-X$^-$ molecular structures found in (**1**)$_2$•Ph$_4$PCl and (**1**)$_2$•Ph$_4$PBr in order to determine a minimal energy geometry (in the gas phase). Starting from the experimental geometry without any constraint led to a minimal energy structure very close to the tetrahedral one (Table 4) for both the chloride and the bromide derivatives. On the other hand, constraining the structures to a square-planar geometry during optimization was unsuccessful, and calculations did not converge.

Table 4. Continuous shape measure calculations giving the $S(G)$ *distance* of the geometry of the six different μ_4-X^- molecular structures shown in Figure 6 to three ideal geometries (See Table S2 in ESI for details).

μ_4-X^- structure	seesaw	tetrahedron	square-planar
$(\mathbf{1})_2 \cdot Ph_4PCl$	1.90	7.09	27.66
$(\mathbf{1})_2 \cdot Cl^-$ (DFT-optimized)	*6.99*	*1.71*	*24.25*
$(\mathbf{1})_2 \cdot Ph_4PBr$ monoclinic	3.24	17.40	9.83
$(\mathbf{1})_2 \cdot Ph_4PBr$ orthorhombic	3.34	17.44	9.67
$(\mathbf{1})_2 \cdot Br^-$ (DFT-optimized)	*7.33*	*2.61*	*23.75*
$\mathbf{2} \cdot Bu_4NCl$	2.03	5.45	26.16
$\mathbf{2} \cdot Bu_4NCl \cdot (PhCN)_{0.5}$			
around Cl(1)	5.95	2.42	27.56
around Cl(2)	4.98	4.81	28.19

Solution NMR studies of the complexation

In order to further investigate the ability of such selenocyanate derivatives to interact with halide anions, we have performed ^1H NMR titrations, where increasing quantities of tetraethylammonium chloride were added to a 0.016M solution of **1** in CDCl$_3$. The CH$_2$ proton singlet resonance exhibits a downfield shift, up to $\Delta\delta = 0.19$ ppm after addition of 4 Cl$^-$ equivalents (Fig S4 in ESI). On the other hand, the signals of the aromatic protons are upfield shifted and split into a complex signal. Based on the methylenic protons, an association constant K$_a$ of 148(1) for the 1:1 complex was determined with the WinEQNMR2[51] program (Fig S4). This value can be compared with those reported earlier, for example in cationic chelating bis-triazolium derivatives bearing SeMe substituents with K$_a$ = 652(13) in CD$_3$CN,[52] or in neutral bis(2-tellurophene)acetylene derivative with K$_a$ = 111 M^{-1} in acetone.[34]

Electrostatic surface potentials (ESP). The different μ_2-X^-, μ_4-X^- structures and NMR studies unambiguously demonstrate the ability of such simple organic selenocyanates to act as chelating ChB donors toward halide anions. Tables 2 and 3 illustrate that the Se•••X^- distances and C–Se•••X^- angles represent strong and directional interactions, with reduction ratio (RR) down

to 0.83, with Cl$^-$ and Br$^-$ anions. The ability of such *ortho*-substituted derivatives **1** or **2** to interact with halides can be also rationalized with calculations of the electrostatic surface potentials (ESP) of the ChB donors. As shown in Figure 7a for the simplest monodentate benzylselenocyanate molecule (BzSeCN), a σ-hole is indeed generated in the prolongation of the NC–Se bond, with a $V_{s,max}$ value of 36.4 kcal mol^{-1}. This $V_{s,max}$ value of 36.4 kcal mol^{-1} in BzSeCN can be also compared with that found, for example, in the prototypical C_6F_5–I XB donor in the same calculation conditions, namely 35.7 kcal mol^{-1}. This further demonstrates that the R–SeCN selenocyanate motif not only exhibits the directionality but also the strength of well-established XB donors. As shown in Figure 7b, when moving from this monodentate benzylselenocyanate to the bidentate ChB donor **1** in its *anti* conformation the σ-holes of both selenium atoms merge into a broad electron-deficient zone characterized by a much larger $V_{s,max}$ value than in BzSeCN, namely 48.3 kcal mol^{-1}. The same calculations performed on the *syn* conformation of the bidentate ChB donor **1** (Figure 7c) similarly provide a broad electron-deficient zone, with an even larger $V_{s,max}$ value, namely 51.5 kcal mol^{-1}. These striking results explain the efficiency of molecules such as **1** or **2** to chelate halide anions. They indeed combine adapted geometrical requirements for chelation with a strongly enhanced electrostatic interaction. They differ in that respect from the many reported chelating systems based on *XB* interactions[2] where halogen atoms are always far apart from each other and do not exhibit such a strong cooperative effect. Similar calculations performed on the tetradentate ChB donor **2** (in its *anti* and its *syn* conformations) give a symmetric picture (Figures S5, S6 in ESI) with two identical, cooperatively enhanced electron-deficient zones with a similarly large $V_{s,max}$ values of 50.2 and 54.6 kcal mol^{-1}, respectively.
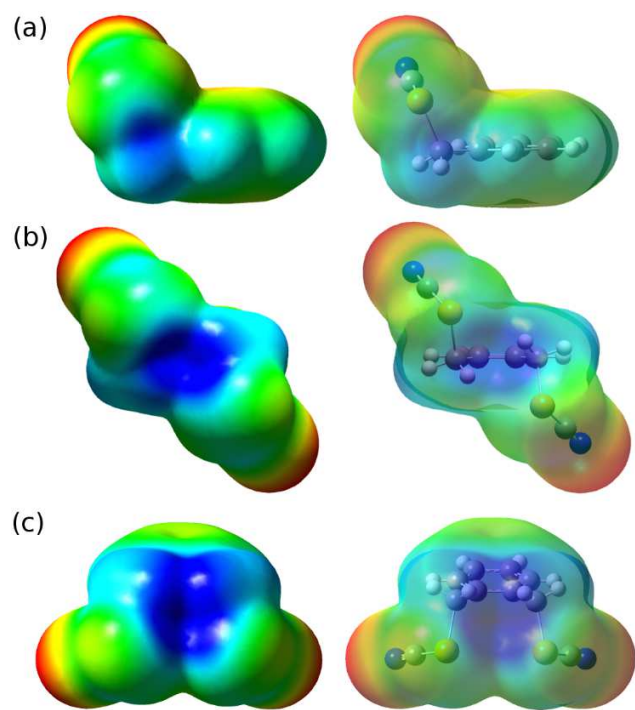
Figure 7. Computed electrostatic potential on the 0.001 a.u. isodensity surface of: (a) benzylselenocyanate BzSeCN, (b) 1,2-bis(selenocyanatomethyl)benzene **1** in *anti* conformation, (c) 1,2-bis(selenocyanatomethyl)benzene **1** in *syn* conformation. Potential scale ranges from –25 kcal mol^{-1} to 38 kcal/mol^{-1}.

CONCLUSIONS

This work provides strong evidence that organic selenocyanates can indeed interact with halide anions in the solid state to form anionic isolated or extended 1D motifs, based on recurrent μ_2- or μ_4-halide structures. The μ_2-halide chalcogen-bonded motifs are characterized here with acute Se•••X$^-$•••Se angles (< 90°), while the μ_4-halide chalcogen-bonded motifs adopt preferentially the so-called seesaw geometry with Br$^-$, and close-to-tetrahedral geometry with Cl$^-$. Both molecules **1** and **2**, with two neighboring SeCN moieties acting as a pincer, either in *syn* or *anti* conformation, generate a broad electron-deficient zone characterized by very large $V_{s,max}$ values of 48–52 kcal mol^{-1} (calculated on the 0.001 a.u. isodensity surface). Shift of solution NMR signals of **1** with increasing amounts of chloride anion confirm the sizeable interaction with a association constant of 148 M^{-1}, demonstrating that such compounds are particularly well suited to act as halide

receptors—a very promising property in light of their involvement in organocatalyzed reactions as well as in biological processes.

EXPERIMENTAL SECTION

Synthesis. 1,2-bis(selenocyanatomethyl)benzene (**1**) and 1,2,4,5-tetrakis (selenocyanatomethyl) benzene (**2**) were prepared as previously described.[53,15] Recrystallization of **1** from DMF with Et_2O layering afforded the **1**•DMF solvate as colourless crystals.

Crystal growth

2•(Ph$_4$PCl)$_2$. In a small tube, **2** (16.1 mg, 0.029 mmol) and Ph$_4$PCl (25.1 mg, 0.067 mmol, 2 equiv) were dissolved in dry benzonitrile (2 mL) at 60°C. After cooling, the solution was layered with dry ether (2 mL) and the tube was left closed for one week, to provide (**2**)•Ph$_4$PCl as slightly orange crystals. Good elemental analysis could not be obtained probably due to contamination with the hydrated form.

2•(Ph$_4$PBr)$_2$. Same procedure as above with **2** (14.6 mg, 0.026 mmol) and Ph$_4$PBr (22.6 mg, 0.054 mmol, 2 equiv). Good elemental analysis could not be obtained probably due to contamination with the hydrated form.

2•(Ph$_4$PCl)$_2$•(H$_2$O)$_2$. Same procedure as above from **2** (16.7 mg, 0.03 mmol) and Ph$_4$PCl (22.4mg, 0.059mmol, 2 equiv), but with one drop of demineralized water added to benzonitrile. M. p. 153°C (decomp.) Elem. Anal. Calcd for **2**•(Ph$_4$PBr)$_2$•(H$_2$O)$_2$ (C$_{62}$H$_{54}$Cl2N$_4$O$_2$P$_2$Se$_4$, MW = 1335.83 g/mol): C, 55.75; H, 4.07; N, 4.19%. Found C, 55.84, H, 4.09, N, 4.08%.

2•(Ph$_4$PBr)$_2$•(H$_2$O)$_2$. Same procedure as above from **2** (10.7 mg, 0.019 mmol) and Ph$_4$PBr (16.4mg, 0.039 mmol, 2 equiv) but with one drop of demineralized water added to benzonitrile. M. p. 171 (decomp). Elem. Anal. Calcd for **2**•(Ph$_4$PBr)$_2$•(H$_2$O)$_2$ (C$_{62}$H$_{54}$Br$_2$N$_4$O$_2$P$_2$Se$_4$, MW = 1424.74 g/mol): C, 52.27; H, 3.82; N, 3.93%. Found C, 52.42, H, 3.73, N, 3.85%.

($\mathbf{1}$)$_2$•Ph$_4$PCl•Et$_2$O. $\mathbf{1}$ (0.0208 g) was dissolved in EtOAc. Ph$_4$PCl (0.0119 g) was added to the EtOAc solution of $\mathbf{1}$, a couple drops of MeOH were added for solubility of the phosphonium salt. Vapor diffusion of ether into the salt solution precipitated white crystals. M. p. 126-127°C (with color change from light orange to gray at 118-120°C). Elem. Anal. Calcd for ($\mathbf{1}$)$_2$•Ph$_4$PCl (C$_{44}$H$_{36}$ClN$_4$PSe$_4$, MW = 1003.0634 g/mol): C, 52.69; H, 3.62; N, 5.59%. Found C, 53.30, H, 3.70, N, 5.32%

($\mathbf{1}$)$_2$•Ph$_4$PBr. $\mathbf{1}$ (0.0193 g) was dissolved in EtOAc. Ph$_4$PBr (0.0128 g) was added to the EtOAc solution of $\mathbf{1}$, a couple drops of MeOH were added for solubility of the phosphonium salt. Vapor diffusion of ether into the salt solution precipitated white crystals. M. p. 133-134°C (with color change from white to gray at 100-110°C). Elem. Anal. Calcd for ($\mathbf{1}$)$_2$•Ph$_4$PBr (C$_{44}$H$_{36}$BrN$_4$PSe$_4$, MW = 1047.5144 g/mol): C, 50.45; H, 3.46; N, 5.35%. Found: C, 50.53, H, 3.35, N, 5.35%.

$\mathbf{2}$•Bu$_4$NCl and $\mathbf{2}$•Bu$_4$NCl•(PhCN)$_{0.5}$. In a small tube, $\mathbf{2}$ (9.5 mg, 0.017 mmol, 1 equiv) and n-Bu$_4$NCl (9.7mg, 0.034mmol, 2 equiv) was dissolved with 2 mL of dry benzonitrile at 60°C and the solution layered with dry ether (2 mL). The tube was tightly closed, and crystals were obtained after one week, as a mixture of the two polymorphs. The intimate mixture hindered elemental analysis or m.p. determination.

Crystallography. Data were collected on an APEXII, Bruker-AXS diffractometer operating with graphite-monochromated Mo-Kα radiation (λ = 0.71073 Å), or on D8 VENTURE Bruker AXS diffractometer at 150 K, operating with graphite-monochromated Mo-Kα radiation (λ = 0.71073 Å) or Cu- Kα radiation (λ = 1.54184 Å). The structures were solved by direct methods using the *SIR92* program,[54] and then refined with full-matrix least-square methods based on F^2 (*SHELXL-2014/7*)[55] with the aid of the WINGX program.[56] All non-hydrogen atoms were refined with anisotropic atomic displacement parameters. H atoms were finally included in their calculated positions. Crystallographic data on X-ray data collection and structure refinements are given in Table S3. CCDC 1865831-1865840 contains the supplementary crystallographic data for this paper.

Theoretical calculations. DFT calculations were performed with the following conditions, with B3LYP functional, 6-31+G** basis set for C, H, N, F and Br, LANDL2Ddp ECP basis set for Se and I, downloaded from the EMSL database.[57,58] Geometry optimization (See Table S4 in ESI for details) was performed for all neutral compounds C_6F_5–I, BzSeCN, *syn*-**1**, *anti*-**1**, and *anti*-**2**, with the exception of *syn*-**2** which is not an energy minimum, and the ESP were computed on the 0.001 a.u. isodensity surfaces. Geometrical optimizations of the μ_4-X^- molecular structure found in (**1**)$_2$•Ph$_4$PCl and (**1**)$_2$•Ph$_4$PBr were performed in the same conditions.

ASSOCIATED CONTENT

Supporting Information

The Supporting Information is available free of charge on the ACS Publications website at DOI: 10.1021/XXX. Pdf file (8 pages) with Figures S1-S5, Tables S1-S4. Crystallographic files in cif format.

Accession Codes CCDC 1865831-1865840 contains the supplementary crystallographic data for this paper. These data can be obtained free of charge via www.ccdc.cam.ac.uk/data_request/cif, or by emailing data_request@ccdc.cam.ac.uk, or by contacting The Cambridge Crystallographic Data Centre, 12, Union Road, Cambridge CB2 1EZ, UK; fax: +44 1223 336033.

AUTHOR INFORMATION

Corresponding Author

*marc.fourmigue@univ-rennes1.fr

ORCID

Marc Fourmigué   https://orcid.org/0000-0002-3796-4802
Orion Berryman   https://orcid.org/0000-0002-0324-484X

Notes

The authors declare no competing financial interest.

18

REFERENCES

[1] Cavallo, G.; Metrangolo, P.; Milani, R.; Pilati, T.; Priimagi, A.; Resnati, G.; Terraneo, G. The Halogen Bond. *Chem. Rev.* **2016***, 116*, 2478–2601.

[2] Gilday, L.C.; Robinson, S.W.; Barendt, T.A.; Langton, M.J.; Mullaney, B.R.; Beer, P.D. Halogen Bonding in Supramolecular Chemistry. *Chem. Rev.* **2015**, *115*, 7118–7195.

[3] Cavallo, G.; Metrangolo, P.; Pilati, T.; Resnati, G.; Terraneo, G. Naming Interactions from the Electrophilic Site. *Cryst. Growth Des*. **2014**, *14*, 2697–2702

[4] Terraneo, G. ; Resnati, G. Bonding Matters. *Cryst. Growth Des*. **2017**, *17*, 1439–1440

[5] Wang, W.; Ji, B.; Zhang, Y. Chalcogen Bond: A Sister Noncovalent Bond to Halogen Bond. *J. Phys. Chem. A* **2009**, *113*, 8132–8135.

[6] Alkorta, I.; Elguero, J.; Del Bene, J. E. A Computational Study of Chalcogen-containing H_2X…YF and $(CH_3)_2X$…YF (X=O, S, Se; Y=F, Cl, H) and Pnictogen-containing H_3X'…YF and $(CH_3)_3X'$…YF (X′=N, P, As) Complexes. *ChemPhysChem* **2018**, DOI:10.1002/cphc.201800179.

[7] Bleiholder, C; Werz, D. B.; Koppel, H; Gleiter, R. Theoretical Investigations on Chalcogen−Chalcogen Interactions: What Makes These Nonbonded Interactions Bonding? *J. Am. Chem. Soc.* **2006**, *128*, 2666–2674.

[8] Politzer, P.; Murray, J. S.; Clark, T.; Resnati, G. The σ-hole revisited. *Phys. Chem. Chem. Phys*. **2017**, *19*, 32166–32178.

[9] Bent, H. A. Structural chemistry of donor-acceptor interactions. *Chem. Rev*. **1968**, *68*, 587–648.

[10] Klapötke, T. M.; Krumm, B.; Scherr, M. Homoleptic Selenium Cyanides: Attempted Preparation of $Se(CN)_4$ and Redetermination of the Crystal Structure of $Se(CN)_2$. *Inorg. Chem.* **2008**, *47*, 7025–7028.

[11] Klapötke, T. M.; Krumm, B.; Gálvez-Ruiz, J. C.; Nöth, H.; Schwab, I. Experimental and Theoretical Studies of Homoleptic Tellurium Cyanides Te(CN)$_x$: Crystal Structure of Te(CN)$_2$. *Eur. J. Inorg. Chem*. **2004**, 4764–4769.

[12] Ho, P. C.; Szydlowski, P.; Sinclair, J.; Elder, P. J. W.; Kübel, J.; Gendy, C.; Lee, L. M.; , Jenkins, H.; Britten, J. F.; Morim, D.; Vargas-Baca, I. Supramolecular macrocycles reversibly assembled by Te…O chalcogen bonding. *Nature Comm*. **2016**, *7*, 11299.

[13] Cozzolino, A. F.; Whitfield, P. S.; Vargas-Baca, I. Supramolecular Chromotropism of the Crystalline Phases of 4,5,6,7-Tetrafluorobenzo-2,1,3-telluradiazole. *J. Am. Chem. Soc*., **2010**, *132*, 17265–17270.

[14] Brezgunova, M.; Lieffrig, J.; Aubert, E.; Dahaoui, S.; Fertey, P.; Lebègue, S.; Angyan, J.; Fourmigué, M.; Espinosa, E. Chalcogen Bonding: Experimental and Theoretical Determinations from Electron Density Analysis. Geometrical Preferences Driven by Electrophilic–Nucleophilic Interactions. *Cryst. Growth Des*. **2013**, *13*, 3283−3289.

[15] Jeannin, O.; Huynh, H.-T.; Riel, A. M. S.; Fourmigué, M. Chalcogen bonding interactions in organic selenocyanates: from cooperativity to chelation. *New J. Chem*. **2018**, *42*, 10502–10509.

[16] Huynh, H.-T.; Jeannin, O.; Fourmigué, M. Organic selenocyanates as strong and directional chalcogen bond donors for crystal engineering. *Chem. Commun.* **2017**, *53*, 8467–8469

[17] Walsh, R. B.; Padgett, C. W.; Metrangolo, P.; Resnati, G.; Hanks, T. W.; Pennington, W. T. Crystal Engineering through Halogen Bonding: Complexes of Nitrogen Heterocycles with Organic Iodides. *Cryst. Growth Des*. **2001**, *1*, 165–175.

[18] Metrangolo, P.; Meyer, F.; Pilati, T.; Resnati, G.; Terraneo, G. 4,4′-Bi-pyridine–2,4,5,6-tetra-fluoro-1,3-di-iodo-benzene (1/1). *Acta Crystallogr*. **2007**, *E63*, o4243.

[19] Mati, S. S.; Roy, S. S.; Chall, S.; Bhattacharya, S.; Bhattacharya, S. C. Unveiling the Groove Binding Mechanism of a Biocompatible Naphthalimide-Based Organoselenocyanate with Calf Thymus DNA: An "Ex Vivo" Fluorescence Imaging Application Appended by Biophysical Experiments and Molecular Docking Simulations. *J. Phys. Chem. B*. **2013**, *117*, 14655–14665.

[20] Facompre, N. D.; El-Bayoumy, K.; Sun Y. W.; Pinto J. T.; Sinha R. 1,4-Phenylene-bis(Methylene)Selenocyanate, but Not Selenomethionine, Inhibits Androgen Receptor and Akt Signaling in Human Prostate Cancer Cells. *Cancer Prev. Res*. **2010**, *3*, 975–984.

[21] Plano, D.; Baquedano, Y.; Moreno-Mateos, D.; Font, M.; Jiménez-Ruiz, A.; Palop, J. A.; Sanmartìn, C. Selenocyanates and diselenides: a new class of potent antileishmanial agents. *Eur. J. Med. Chem.* **2011**, *46*, 3315–3323.

[22] Cavallo, G.; Metrangolo, P.; Pilati, T.; Resnati, G.; Sansotera, M.; Terraneo, G. Halogen bonding: a general route in anion recognition and coordination. *Chem. Soc. Rev.* **2010**, *39*, 3772–3783.

[23] Metrangolo, P.; Meyer, F.; Pilati, T.; Resnati, G.; Terraneo, G. Halogen Bonding in Supramolecular Chemustry. *Angew. Chem. Int. Ed.* **2008**, *47*, 6114–6127.

[24] Lieffrig, J.; Jeannin, O.; Frąckowiak, A.; Olejniczak, I.; Świetlik, R.; Dahaoui, S.; Aubert, E.; Espinosa, E.; Auban-Senzier, P.; Fourmigué, M. Charge-Assisted Halogen Bonding: Donor–Acceptor Complexes with Variable Ionicity. *Chem. Eur. J.* **2013**, *19*, 14804–14813.

[25] Riel, A. M. S.; Decato, D. A.; Sun, J.; Massena, C. J.; Jessop, M. J.; Berryman, O. B. The intramolecular hydrogen bonded–halogen bond: a new strategy for preorganization and enhanced binding. *Chem. Sci.* **2018,** 9, 5828–5836.

[26] Wageling, N. B.; Neuhaus, G. F.; Rose, A. M.; Decato, D. A.; Berryman, O. B. Advantages of organic halogen bonding for halide recognition. *Supramol. Chem.* **2016,** 28, 665–672.

[27] Massena, C. J.; Wageling, N. B.; Decato, D. A.; Martin Rodriguez, E.; Rose, A. M.; Berryman, O. B. A Halogen-Bond-Induced Triple Helicate Encapsulates Iodide. *Angew. Chem. Intl. Ed.*, **2016**, 55, 12398–12402.

[28] Fourmigué, M. Coordination chemistry of anions through halogen-bonding interactions. *Acta Cryst.* **2017**, *B73*, 138–139.

[29] Lieffrig, J.; Jeannin, O.; Fourmigué, M. Expanded Halogen-Bonded Anion Organic Networks with Star-Shaped Iodoethynyl-Substituted Molecules: From Corrugated 2D Hexagonal Lattices to Pyrite-Type 2-Fold Interpenetrated Cubic Lattices. *J. Am. Chem. Soc.* **2013**, *135*, 6200–6210.

[30] Viger-Gravel, J.; Leclerc, S.; Korobkov, I.; Bryce, D. L. Correlation between ^{13}C chemical shifts and the halogen bonding environment in a series of solid *para*-diiodotetrafluorobenzene complexes. *CrystEngComm* **2013**, *15*, 3168–3177.

[31] Szell, P. M. J.; Cavallo, G.; Terraneo, G.; Metrangolo, P.; Gabidullin, B.; Bryce, D. L. Comparing the Halogen Bond to the Hydrogen Bond by Solid-State NMR Spectroscopy:

Anion Coordinated Dimers from 2- and 3-Iodoethynylpyridine Salts. *Chem. Eur. J.* **2018**, 24, 11364–11376.

[32] Szell, P. M. J.; Gabidullin, B.; Bryce, D. L. 1,3,5-Tri(iodoethynyl)-2,4,6-tri-fluoro-benzene: halogen-bonded frameworks and NMR spectroscopic analysis. *Acta Cryst. B*, **2017**, *73*, 153–162.

[33] Schmidt, B.; Sonnenberg, K.; Beckers, H.; Steinhauser, S.; Riedel, S. Synthesis and Characterization of Nonclassical Interhalides Based on Bromine Monochloride. *Angew. Chem. Int. Ed.* **2018**, *57*, 9141–9145.

[34] Garrett, G. E.; Carrera, E. I.; Seferos, D. S.; Taylor, M. S. Anion recognition by a bidentate chalcogen bond donor. *Chem. Commun*. **2016**, *52*, 9881–9884.

[35] Garrett, G. E.; Gibson, G. L.; Straus, R. N.; Seferos, D. S.; Taylor, M. S. Chalcogen Bonding in Solution: Interactions of Benzotelluradiazoles with Anionic and Uncharged Lewis Bases. *J. Am. Chem. Soc*. **2015**, 137, 4126–4133.

[36] Scheiner, S. Highly Selective Halide Receptors Based on Chalcogen, Pnicogen, and Tetrel Bonds. *Chem. Eur. J.* **2016**, *22*, 18850–18858.

[37] Scheiner, S. Comparison of halide receptors based on H, halogen, chalcogen, pnicogen, and tetrel bonds. *Faraday Discuss*. **2017**, *203*, 213–226.

[38] Benz, S.; Macchione, M.; Verolet, Q.; Mareda, J.; Sakai, N.; Matile, S. Anion Transport with Chalcogen Bonds. *J. Am. Chem. Soc*. **2016**, *138*, 9093–9096.

[39] Sánchez-Sanz, G.; Trujillo, C. Improvement of Anion Transport Systems by Modulation of Chalcogen Interactions: The influence of solvent. *J. Phys. Chem. A* **2018**, *122*, 1369–1377.

[40] Macchione, M.; Tsemperouli, M.; Goujon, A.; Mallia, A. R.; Sakai, N.; Sugihara, K.; Matile, S. Mechanosensitive Oligodithienothiophenes: Transmembrane Anion Transport Along Chalcogen-Bonding Cascades. *Helv. Chim. Acta* **2018**, *101*, e1800014.

[41] Lim, J. Y. C.; Marques, I.; Thompson, A. L.; Kirsten E. Christensen, K. E.; Félix, V., Beer, P. D. Chalcogen Bonding Macrocycles and [2]Rotaxanes for Anion Recognition. *J. Am. Chem. Soc.* **2017**, *139*, 3122–3133.

[42] Benz, B.; Lopez-Andarias, J.; Mareda, J.; Sakai, N. Matile, S. Catalysis with Chalcogen Bonds. *Angew. Chem. Int. Ed*. **2017**, 56, 812 –815.

[43] Benz, S.; Mareda, J.; Besnard, C.; Sakai, N; Matile, S. Catalysis with chalcogen bonds: neutral benzodiselenazole scaffolds with high-precision selenium donors of variable strength. *Chem. Sci*. **2017**, *8*, 8164-8169

[44] Wonner, P.; Vogel, L.; Düser, M.; Gomes, L.; Kniep, F.; Mallick, B.; Werz, D. B.; Huber, S. M. Carbon-Halogen Bond Activation by Selenium-Based Chalcogen Bonding. *Angew. Chem. Int. Ed*. **2017**, *56*, 12009 –12012.

[45] Wonner, P.; Vogel, L.; Kniep, F.; Huber, S. M. Catalytic Carbon–Chlorine Bond Activation by Selenium-Based Chalcogen Bond Donors. *Chem. Eur. J*. **2017**, *23*, 16972–16975.

[46] Hauge, S.; Maroy, K. Reactions between Selenocyanate and Bromine. Syntheses and Crystal Structures of Phenyltrimethylammonium Salts of Dibromoselenocyanate, $[C_6H_5(CH_3)_3N][SeCNBr_2]$, and Bromodiselenocyanate, $[C_6H_5(CH_3)_3N][(SeCN)_2Br]$. *Acta Chem. Scand*. **1992**, *46*, 1166–1169.

[47] Semenov, N. A.; Gorbunov, D. E.; Shakhova, M. V.; Salnikov, G. E.; Bagryanskaya, I. Y.; Korolev, V. V.; Beckmann, J.; Gritsan, N. P.; Zibarev, A. V. Donor–Acceptor Complexes between 1,2,5-Chalcogenadiazoles (Te, Se, S) and the Pseudohalides CN^- and XCN^- (X=O, S, Se, Te). *Chem. Eur. J*. **2018**, 24, 12983–12991.

[48] Kumar, V; Leroy, C.; Bryce, D. L. Halide ion recognition via chalcogen bonding in the solid state and in solution. Directionality and linearity. *CrystEngComm* **2018**, *20*, 6406–6411.

[49] Cirera, J.; Alemany, P.; Alvarez, S. Mapping the Stereochemistry and Symmetry of Tetracoordinate Transition-Metal Complexes. *Chem. Eur. J*. **2004**, *10*, 190–207.

[50] Alvarez, S.; Alemany, P.; Casanova, D.; Cirera, J.; Llunell, M.; Avnir, D. Shape Maps and Polyhedral Interconversion Paths in Transition Metal Chemistry. *Coord. Chem. Rev*. **2005**, *249*, 1693–1708.

[51] Hynes, M. J. EQNMR: a computer program for the calculation of stability constants from nuclear magnetic resonance chemical shift data. *J. Chem. Soc., Dalton Trans*. **1993**, 311−312.

[52] Lim, J. Y. C.; Liew, J. Y. Beer, P. D. Thermodynamics of Anion Binding by Chalcogen Bonding Receptors. *Chem. Eur. J*. **2018**, 24, 14560–14566.

[53] McWhinnie, S. L. W.; Brooks, A. B.; Abrahams, I. αα'-Di-seleno-cyanato-ortho-xylene. *Acta Cryst. C*, **1998**, *54*, 126–128.

[54] Altomare, A.; Cascarano, G.; Giacovazzo, C.; Guagliardi, A.; Burla, M. C.; Polidori, G.; Camalli, M. SIR92 – a program for automatic solution of crystal structures by direct methods. *J. Appl. Cryst.* **1994**, *27*, 435–436.

[55] Sheldrick, G. M. Crystal structure refinement with SHELXL. *Acta Cryst. C*, **2015**, *71*, 3–8.

[56] Farrugia, L. J. WinGX and ORTEP for Windows: an update. *J. Appl. Cryst.* **2012**, *45*, 849–854.

[57] Feller, D. The role of databases in support of computational chemistry calculations. *J. Comp. Chem*. **1996**, *17*, 1571–1586.

[58] Schuchardt, K.L., Didier, B.T., Elsethagen, T., Sun, L., Gurumoorthi, V., Chase, J., Li, J., and Windus, T.L. Basis set exchange: a community database for computational sciences. *J. Chem. Inf. Model.* **2007**, *47*, 1045–1052.

Organic selenocyanates as halide receptors: from chelation to one-dimensional systems

Asia Marie S. Riel,[†,‡] Huu-Tri Huynh,[†] Olivier Jeannin,[†] Orion Berryman,[‡] and Marc Fourmigué*,[†]

[†] Univ Rennes, CNRS, ISCR (Institut de Sciences Chimiques de Rennes), UMR 6226, 35000 Rennes, France

[‡] Department of Chemistry and Biochemistry, University of Montana, 32 Campus Dr., Missoula MT 59812, USA

For Table of Contents Use Only

Ortho-substituted bis(selenocyanatomethyl)benzene derivatives act as efficient chelating agents for halides through short and directional Se•••X⁻ chalcogen bonding (ChB) interactions. Crystal structures of μ_2-halide and μ_4-halide motifs are analyzed, together with complementary ^{1}H solution NMR studies and theoretical calculations.